Journal of Zhejiang University-SCIENCE B (Biomedicine & Biotechnology) 2023 24(6):496-509
www.jzus.zju.edu.cn; www.springer.com/journal/11585
E-mail: jzus_b@zju.edu.cn

Research Article

https://doi.org/10.1631/jzus.B2200674

Engineered *Bacillus subtilis* alleviates intestinal oxidative injury through Nrf2-Keap1 pathway in enterotoxigenic *Escherichia coli* (ETEC) K88-infected piglet

Chaoyue WEN[1], Hong ZHANG[1], Qiuping GUO[2], Yehui DUAN[2], Sisi CHEN[2,3], Mengmeng HAN[2,3], Fengna LI[2], Mingliang JIN[1]✉, Yizhen WANG[1]✉

[1]*Institute of Feed Science, Key Laboratory of Animal Feed and Nutrition of Zhejiang Province, Key Laboratory of Molecular Animal Nutrition, Ministry of Education, Key Laboratory of Animal Nutrition and Feed Science in Eastern China, Ministry of Agriculture, College of Animal Sciences, Zhejiang University, Hangzhou 310058, China*
[2]*Hunan Provincial Key Laboratory of Animal Nutritional Physiology and Metabolic Process, CAS Key Laboratory of Agro-Ecological Processes in Subtropical Region, National Engineering Laboratory for Pollution Control and Waste Utilization in Livestock and Poultry Production, Institute of Subtropical Agriculture, Chinese Academy of Sciences, Changsha 410125, China*
[3]*College of Advanced Agricultural Science, University of Chinese Academy of Sciences, Beijing 100039, China*

Abstract: Engineered probiotics can serve as therapeutics based on their ability of produce recombinant immune-stimulating properties. In this study, we built the recombinant *Bacillus subtilis* WB800 expressing antimicrobial peptide KR32 (WB800-KR32) using genetic engineering methods and investigated its protective effects of nuclear factor-E2-related factor 2 (Nrf2)-Kelch-like ECH-associated protein 1 (Keap1) pathway activation in intestinal oxidative disturbance induced by enterotoxigenic *Escherichia coli* (ETEC) K88 in weaned piglets. Twenty-eight weaned piglets were randomly distributed into four treatment groups with seven replicates fed with a basal diet. The feed of the control group (CON) was infused with normal sterilized saline; meanwhile, the ETEC, ETEC+WB800, and ETEC+WB800-KR32 groups were orally administered normal sterilized saline, 5×10^{10} CFU (CFU: colony forming units) WB800, and 5×10^{10} CFU WB800-KR32, respectively, on Days 1–14 and all infused with ETEC K88 1×10^{10} CFU on Days 15–17. The results showed that pretreatment with WB800-KR32 attenuated ETEC-induced intestinal disturbance, improved the mucosal activity of antioxidant enzyme (catalase (CAT), superoxide dismutase (SOD), and glutathione peroxidase (GPx)) and decreased the content of malondialdehyde (MDA). More importantly, WB800-KR32 downregulated genes involved in antioxidant defense (GPx and SOD1). Interestingly, WB800-KR32 upregulated the protein expression of Nrf2 and downregulated the protein expression of Keap1 in the ileum. WB800-KR32 markedly changed the richness estimators (Ace and Chao) of gut microbiota and increased the abundance of *Eubacterium_rectale_ATCC_33656* in the feces. The results suggested that WB800-KR32 may alleviate ETEC-induced intestinal oxidative injury through the Nrf2-Keap1 pathway, providing a new perspective for WB800-KR32 as potential therapeutics to regulate intestinal oxidative disturbance in ETEC K88 infection.

Key words: Engineered probiotics; Intestine; Oxidative injury; Weaned piglets; Nuclear factor-E2-related factor 2 (Nrf2)-Kelch-like ECH-associated protein 1 (Keap1) pathway

1 Introduction

Enterotoxigenic *Escherichia coli* (ETEC) is a common pathogen of the gut microbiota, causing diarrhea both in humans and animals, especially in the neonatal and suckling periods (Luise et al., 2019). It has been reported that ETEC can damage the epithelial barrier, increase intestinal permeability (Tang et al., 2014), induce apoptotic processes (Xia et al., 2018, 2019), and disturb the harmony of gut flora (Xie et al., 2021). As gut microbes will affect the future growth and health of the host (Bäckhed et al., 2012; Xie et al., 2021), it is essential to maintain their homeostasis. ETEC infection is characterized by the imbalance of intestinal antioxidant homeostasis, with reduced activity of

✉ Yizhen WANG, yzwang321@zju.edu.cn
Mingliang JIN, mljin@zju.edu.cn
Yizhen WANG, https://orcid.org/0000-0002-3908-7102
Mingliang JIN, https://orcid.org/0000-0001-6358-5307

Received Dec. 27, 2022; Revision accepted Mar. 1, 2023; Crosschecked May 16, 2023

antioxidant enzymes such as glutathione peroxidase (GPx) and superoxide dismutase (SOD), the upregulation of inflammatory responses, and downregulation of antioxidant genes in the intestine (Yu et al., 2021). It is universally acknowledged that the use of antibiotics constitutes the conventional means to treat pathogen infections. However, due to the food safety reasons and to prevent the development of resistant strains, antibiotics are being phased out from animal feeds (Wierup, 2001; Lekshmi et al., 2017). Consequently, the exploration of new strategies to prevent pathogen infections is extremely urgent.

The antimicrobial peptide (AMP) KR32 was designed in our laboratory based on cathelicidin-BF, a natural AMP derived from snake venom (Hu et al., 2019; Liu et al., 2019). It exhibited high antimicrobial activity with minimal hemolytic activity and cytotoxicity (Hu et al., 2019). Subsequent studies confirmed that KR32 alleviates diarrhea on post-weaning piglets and decreases the level of inflammatory cytokines (Hu et al., 2019). However, it is time-consuming and costly to synthesize and purify AMPs (Luan et al., 2014a, 2014b). Bioengineered probiotics have been demonstrated to be effective against pathogens that commonly infect the gut (Cruz et al., 2022). *Bacillus subtilis* has been considered safe by the United States Food and Drug Administration, which acts as a superb delivery vehicle to produce AMPs (Luan et al., 2014a). Additionally, this species has a naturally large secretory capacity and exports proteins directly into the extracellular medium (Li et al., 2004). Therefore, we constructed a plasmid based on pBE2R, which is a composition-type plasmid for producing AMP KR32 in the *B. subtilis* expression system.

In this study, we used *B. subtilis* as a delivery vehicle by developing a recombinant strain expressing KR32. The nuclear factor-E2-related factor 2 (Nrf2)-Kelch-like ECH-associated protein 1 (Keap1) signaling pathway is important in resistance to oxidative stress in the intestine (Rajput et al., 2021; Shi et al., 2022; Huang et al., 2023). Nrf2 is an oxidation-reduction-sensitive transcription factor that stimulates antioxidant enzyme expression, thus moderating oxidative injury (Younis et al., 2020; Wang et al., 2022). Piglets were selected as the model for the similarity of their gastrointestinal tract structure and function to those of human beings (Guilloteau et al., 2010; Zhang et al., 2013; Roura et al., 2016). We aimed to validate the hypothesis that recombinant *B. subtilis* WB800-pBE2R-KR32 could improve intestinal antioxidant capacity induced by ETEC K88 infection via the Nrf2-Keap1 pathway. Based on the findings, the present study provides a scientific basis for treating ETEC-induced impaired intestinal antioxidant capacity in humans and piglets.

2 Materials and methods

2.1 Bacterial strains

DH5α cells stored in our lab were used for subcloning and plasmid amplification. The *B. subtilis* WB800 strain (Forhigh Biotech, China) was utilized as the expression host, grown in Luria-Bertani (LB) broth (Sangon, Shanghai, China) at 37 °C. The shuttle vector pBE2R (MiaoLing Plasmid Platform) was employed for the secretion of target protein (peptide). T4 DNA ligase, Taq DNA polymerase, and all restriction enzymes were purchased from New England Biolabs (Beverly, MA, USA). The *KR32* gene was synthesized and inserted into the pBE2R vector by MiaoLing Plasmid Platform (Wuhan, China). The map of the obtained recombinant plasmid pBE2R-KR32 was shown in Fig. S1. This plasmid was then electro-transformed into competent WB800, which was further plated on LB plates (with 50 μg/mL kanamycin) for positive selection to generate *B. subtilis* WB800-pBE2R-KR32 (WB800-KR32). *B. subtilis* WB800 transformed with pBE2R plasmid was used as negative control. The *E. coli* K88 strain used in this study was available from our lab (Hu et al., 2019) and was cultured in LB broth containing 1% (10 g/L) tryptone, 0.5% (5 g/L) yeast extract, and 1% (10 g/L) NaCl at pH 7.0 for 12 h to reach saturation ($\geqslant 1.0\times10^8$ CFU/mL; CFU: colony forming units). The bacterial cells were harvested by centrifugation at 3000*g* for 10 min at 4 °C, washed, and suspended in sterile saline. A solution of ETEC K88 strain containing about 1×10^9 CFU/mL was prepared.

2.2 Animals and experimental design

All animal procedures were approved by the Committee of the Institute of Subtropical Agriculture, the Chinese Academy of Sciences (No. ISA-2022-022). Twenty-eight Duroc×Landrace×Yorkshire piglets weaned at 21 d were caged in individual pens. After 3 d of adaption, the piglets ((7.09±0.25) kg) were randomly allocated into four groups (Fig. 1) (n=7 per

treatment): (1) oral administration of 10 mL 0.9% (9 g/L) NaCl (CON group); (2) oral administration of 10 mL 0.9% NaCl+ETEC challenge (ETEC group); (3) oral administration of 10 mL 5.0×10^9 CFU/mL WB800 bacteria solution+ETEC challenge (ETEC+WB800 group); (4) oral administration of 10 mL 5.0×10^9 CFU/mL WB800-KR32 bacteria solution+ETEC challenge (ETEC+WB800-KR32 group). On Day 15 08:00 a.m., all piglets were weighed. ETEC (1×10^9 CFU/mL, 10 mL) was orally administered to animals in the ETEC challenge group once a day for three days from Days 15 to 17. The cytokines (interleukin-6 (IL-6) and IL-1β) were increased significantly after three days of treatment with ETEC (Ren et al., 2019). The doses and durations of ETEC K88 were set according to a previous study (Ren et al., 2019). Piglets in the CON group were administered with 10 mL 0.9% NaCl.

2.3 Sample collection

Fecal samples were collected on Days 1, 14, and 17 from animals in the ETEC+WB800-KR32 group. The collected samples were stored at −80 °C until further analysis. On Day 15, prior to ETEC infection, blood samples were taken and centrifuged at 3000*g* for 10 min, and then kept at −20 °C until further analysis. On Day 17, after 12 h of fasting, all piglets were weighed to evaluate the post-challenge growth performance, and blood samples were collected via vein puncture and then centrifuged at 3000*g* for 10 min. The supernatants were collected and stored at −20 °C until further analysis. Finally, all piglets were slaughtered via electrical stunning (250 V, 0.5 A, 5–6 s) and bled by the exsanguination of precaval vein. The mucosae of duodenum, jejunum, and ileum were collected immediately, quickly frozen in liquid N_2, and stored at −80 °C until further analysis.

2.4 Analysis of serum and intestinal antioxidant parameters

Catalase (CAT), malondialdehyde (MDA), SOD, GPx, and total antioxidant capacity (T-AOC) in the serum and intestinal (duodenum, jejunum, and ileum) mucosa were measured using commercial kits (Hunan AiFang biological, Changsha, China).

2.5 Gene expression analysis

Quantitative real-time polymerase chain reaction PCR (qPCR) was performed as described previously (Li et al., 2015; Duan et al., 2017; Wen et al., 2019). Total RNAs of jejunal and ileal mucosae were extracted using the TRIzol reagent (Beyotime Biotechnology, Shanghai, China). The primers for the target genes were listed in Table 2. *β-actin* was used as the housekeeping gene to normalize the expression of target genes. The expression levels of target genes were determined by the $2^{-\Delta\Delta C_T}$ method.

2.6 Western blotting analysis

The relative protein levels for Nrf2 and Keap1 were measured by western blotting according to our previous studies (Wen et al., 2020a, 2020b). The primary antibodies used in our study included anti-Nrf2, anti-Keap1, and mouse anti-β-actin. All the antibodies were purchased from ABclonal Technology (ABclonal Technology, Wuhan, China). The acquired signals were visualized via ChemiScope 6100 (Clinx, Shanghai, China).

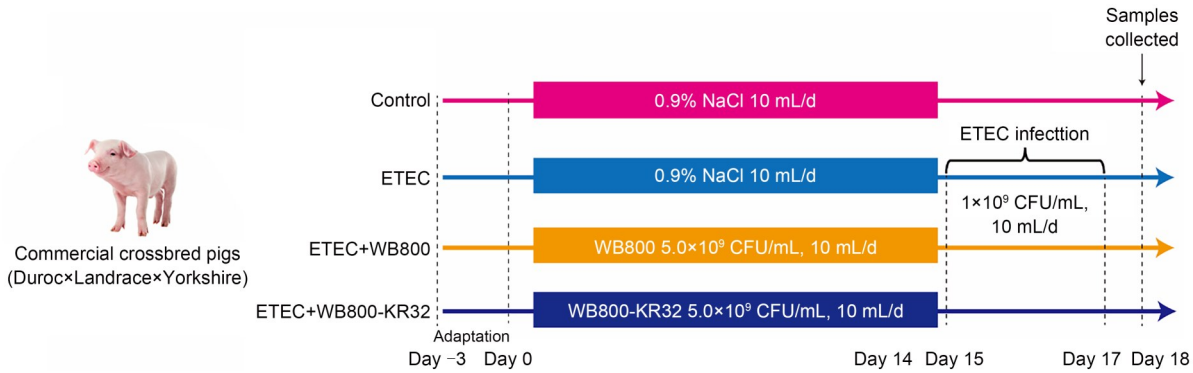

Fig. 1 Schematic of the experimental design of the animal treatments. A corn-soybean meal diet (Table 1) was formulated according to the Nutrient Requirements of Swine (National Research Council, 2012). All piglets had access to water and feed ad libitum. ETEC: enterotoxigenic *Escherichia coli*; CFU: colony forming units.

Table 1 Ingredients and chemical compositions of the experimental diets

Composition	Proportion (%)*
Ingredients	
Corn meal	59.88
Soybean meal	24.45
Fish meal	4.99
Dried whey	3.99
Soybean oil	2.00
Lysine	0.48
Methionine	0.09
Threonine	0.16
Tryptophan	0.04
NaCl	0.30
$CaHPO_4$	0.95
Glucose	0.80
Limestone	0.79
Premix[a]	1.09
Nutrient content	
Digestible energy (MJ/kg)	14.56
Crude protein	19.31
SID lysine	1.28
SID methionine+cysteine	0.64
SID threonine	0.77
SID tryptophan	0.23
Total calcium	0.85
Total phosphorus	0.63
Digestible phosphorus	0.39

* All data are expressed in g/100 g dry mass except for digestible energy in MJ/kg. [a] Supplied in per kg of diet: $CuSO_4 \cdot 5H_2O$, 19.8 mg; KI, 0.20 mg; $FeSO_4 \cdot 7H_2O$, 400 mg; $NaSeO_3$, 0.56 mg; $ZnSO_4 \cdot 7H_2O$, 359 mg; $MnSO_4 \cdot H_2O$, 10.2 mg; vitamin K (menadione), 5 mg; vitamin B1, 2 mg; vitamin B2, 15 mg; vitamin B12, 30 μg; vitamin A, 5400 IU; vitamin D3, 110 IU; vitamin E, 18 IU; choline chloride, 80 mg; antioxidants: ethoxyquin, 20 mg. SID: standardized ileal digestible.

2.7 Analysis of fecal microbiota

The microbial community DNA of fecal contents was extracted using the MagPure Stool DNA KF Kit B (Magen, China). The V3–V4 variable region of the bacterial 16S ribosomal RNA (rRNA) gene was amplified with degenerate PCR primers (341F, 5'-ACTCCTACGGGAGGCAGCA-3'; 806R, 5'-GGACTACHVGGGTWTCTAAT-3') and sequenced on the Illumina MiSeq platform (BGI, Shenzhen, China). The assembled MiSeq sequences were uploaded to the Sequence Read Archive of the National Center for Biotechnology Information (NCBI, Sequence Read Archive (SRA) BioProject No. PRJNA894787). The raw reads were filtered and assembled according to described protocols (Zhou et al., 2019; Wen et al., 2021). The data were analyzed as previously described (Jin et al., 2018). Briefly, to investigate bacterial richness and diversity, alpha-diversity was estimated by Mothur (v. 1.30.2; https://mothur.org), including the Sobs, Chao, Ace, Shannon, and Simpson indices. Beta-diversity was estimated by Quantitative Insights Into Microbial Ecology (QIIME, v. 1.8.0; http://qiime.org/1.8.0) at the operational taxonomic unit (OTU) level by calculating Bray-Curtis dissimilarity, and then visualized by principal coordinate analysis (PCoA) and non-metric multi-dimensional scaling (NMDS). Kruskal-Wallis H-test was performed to estimate the significant differences between species. The Kyoto Encyclopedia of Genes and Genomes (KEGG) functions were predicted by Phylogenetic Investigation of Communities by Reconstruction of Unobserved States (PICRUSt) software (v.1.1.0; http://picrust.github.io/picrust).

Table 2 Characteristics of the primers used for real-time PCR analysis

Gene	Sequence (5'→3')	Accession No.	Size (bp)
CAT	F: CTCACAGCGAATACCCTC R: TGTTCAACCTCAGCAAAA	NC_010444.4	82
SOD1	F: GAGACCTGGGCAATGTGACT R: CCAAACGACTTCCAGCATTT	NC_010455.5	189
Keap1	F: TCAACCGTCTGCTCTACG R: CACTCATTCCTCTCTGGG	NC_010444.3	465
Nrf2	F: GAAAGCCCAGTCTTCATTGC R: TTGGAACCGTGCTAGTCTCA	NC_010457.5	190
GPx	F: AGCCCAACTTCATGCTCTTC R: CATTGCGACACACTGGAGAC	NC_010455.5	159
β-actin	F: TGCGGGACATCAAGGAGAAG R: AGTTGAAGGTGGTCTCGTGG	NC_010445.4	216

CAT, catalase; *SOD1*, superoxide dismutase 1; *Keap1*, Kelch-like ECH-associated protein 1; *Nrf2*, nuclear factor erythroid 2-related factor 2; *GPx*, glutathione peroxidase.

2.8 Statistical analysis

All results were expressed as mean±standard error of the mean (SEM). Serum biochemistry index data were analyzed using *t*-test. Other data were analyzed using one-way analysis of variance (ANOVA) followed by Duncan's multiple comparison test using SAS 8.2 software (SAS Institute, NC, USA). Probability values of <0.05 were considered statistically significant.

3 Results

3.1 Serum biochemical index

Prior to ETEC infection, oral WB800-KR32 showed no significant effects on the serum biochemical indices, including albumin (ALB), alkaline phosphatase (ALP), acid phosphatase 2 (ACP2), alanine aminotransferase (ALT), creatine kinase (CK), and immunoglobulin M (IgM). No significant differences were found between before and after infection, and therefore changes were not attributable to ETEC (Table 3).

3.2 Serum and intestine antioxidant parameters

Compared with the CON group, the activity of CAT and T-AOC was significantly decreased in the ETEC and ETEC+WB800 groups (P<0.05; Figs. 2a and 2e). However, pretreatment with WB800-KR32 elevated the activity of CAT and T-AOC upon ETEC infection in the serum (P<0.05). Relative to the ETEC group, the activity of SOD was significantly increased in the duodenum (P<0.05; Fig. 2j). Relative to the CON group, ETEC infection decreased both T-AOC and the activity of GPx in the jejunum and ileum (P<0.05; Figs. 2g, 2h, 2s, and 2t). Interestingly, these decrements caused by ETEC infection except for T-AOC in ileum were reversed by WB800-KR32 infusion. What is more, the content of MDA was significantly increased in the ETEC group in the jejunum, while the change was alleviated by WB800-KR32 treatment (P<0.05; Fig. 2o).

Table 3 Effects of oral WB800-KR32 on the serum biochemical indices of weaned pigs (pre- and post-infection)

Treatment	ALB (U/L)	ALP (U/L)	ACP2 (U/L)	ALT (U/L)	CK (U/L)	IgM (g/L)
Prior to ETEC K88 infection						
CON	28.20±2.41	341.57±50.65	24.96±4.25	46.34±8.97	585.43±94.59	0.40±0.04
ETEC	32.60±2.05	426.57±30.36	21.86±4.51	43.73±1.89	338.83±57.31	0.42±0.04
WB800	32.11±1.42	351.43±29.30	25.71±5.18	48.09±6.54	607.14±189.98	0.44±0.04
WB800-KR32	30.16±2.37	344.14±30.36	30.48±3.03	50.61±5.40	468.00±85.52	0.38±0.03
After ETEC K88 infection						
CON	30.31±1.37	323.14±49.85	31.10±4.19	49.15±7.45	766.00±240.95	0.55±0.11
ETEC	31.74±1.51	291.29±19.88	22.50±3.85	43.17±1.95	662.50±105.74	0.54±0.06
ETEC+WB800	30.89±0.65	275.86±26.13	26.86±5.17	45.18±4.65	482.83±84.89	0.57±0.06
ETEC+WB800-KR32	28.20±1.83	272.86±29.30	28.46±3.36	49.91±3.58	442.83±31.50	0.46±0.03
P-value						
P_a	0.45	0.31	0.57	0.88	0.42	0.73
P_b	0.35	0.70	0.54	0.68	0.67	0.28
P_1	0.35	0.08	0.80	0.20	0.32	0.23
P_2	0.70	0.89	0.12	0.07	0.85	0.08
P_3	0.69	0.06	0.08	0.70	0.88	0.07
P_4	0.92	0.96	0.12	0.57	0.66	0.10

The results were expressed as mean±standard error of the mean (SEM), n=7. CON, basal diet infused with sterilized normal saline; ETEC, infected control (piglets receiving a basal diet plus oral dose infused with enterotoxigenic *Escherichia coli* (ETEC) K88); ETEC+WB800, piglets receiving a basal diet plus oral dose infused with 1×10^{10} CFU (CFU: colony forming units) WB800 and ETEC K88; ETEC+WB800-KR32, piglets receiving a basal diet plus oral dose infused with 1×10^{10} CFU WB800-KR32 and ETEC K88. ALB, albumin; ALP, alkaline phosphatase; ACP2, acid phosphatase 2; ALT, alanine aminotransferase; CK, creatine kinase; IgM, immunoglobulin M. P_a: multivariate analysis of variance in prior to ETEC K88 infection; P_b: multivariate analysis of variance in post to ETEC K88 infection; P_1: prior to ETEC K88 infection (CON) vs. post-ETEC K88 infection (CON); P_2: prior to ETEC K88 infection (CON) vs. post-ETEC K88 infection (ETEC); P_3: prior to ETEC K88 infection (WB800) vs. post-ETEC K88 infection (ETEC+WB800); P_4: prior to ETEC K88 infection (WB800-KR32) vs. post-ETEC K88 infection (ETEC+WB800-KR32).

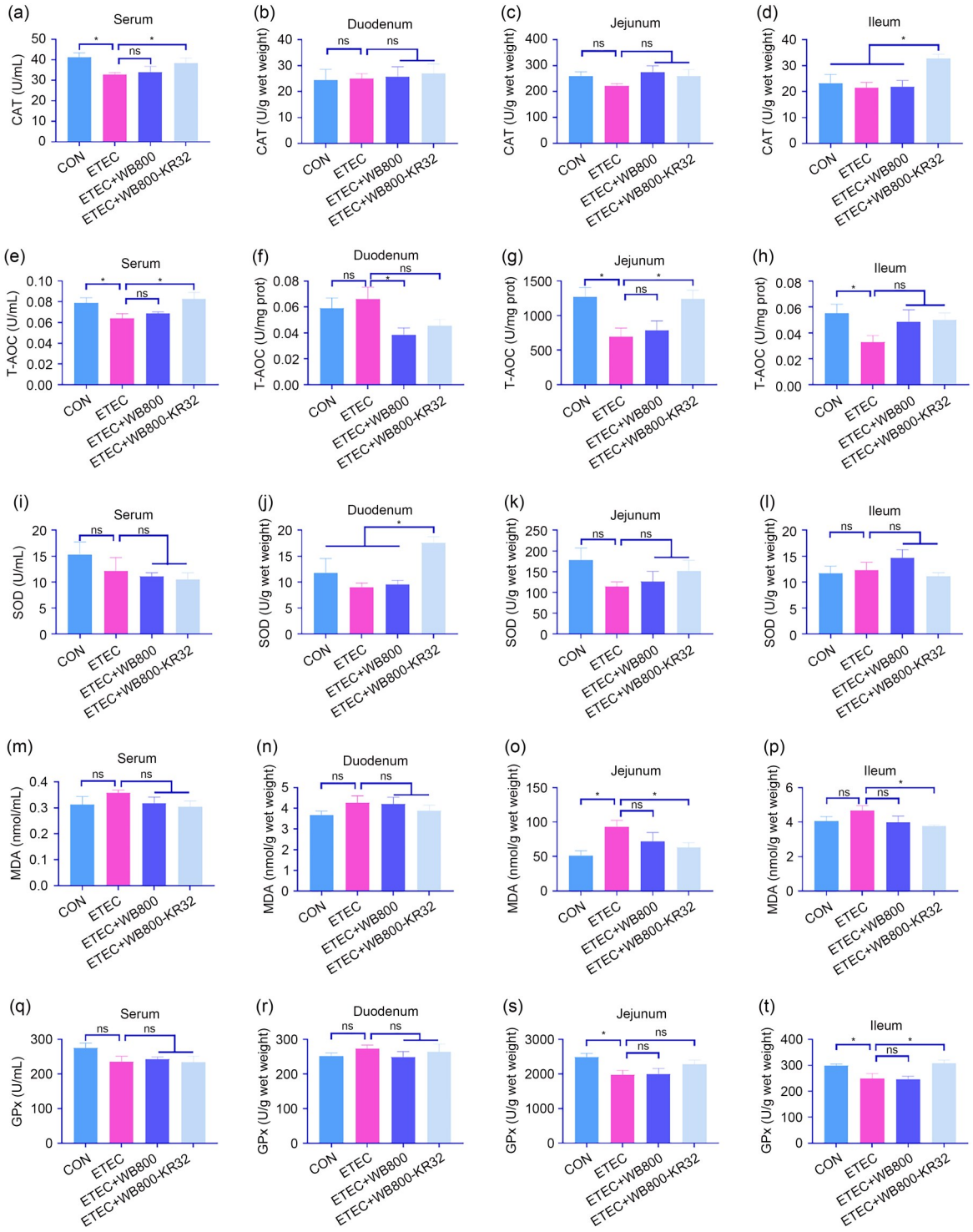

Fig. 2 Effects of WB800-KR32 on the serum antioxidant activity (a, e, i, m, q) and the mucosae of duodenum (b, f, j, n, r), jejunum (c, g, k, o, s), and ileum (d, h, l, p, t) in weaned piglets infected with ETEC K88. The results were expressed as mean±standard error of the mean (SEM), n=7. * P<0.05, ^{ns} P>0.1. CON, basal diet infused with sterilized normal saline; ETEC, infected control (piglets receiving a basal diet plus oral dose infused with ETEC K88); ETEC+WB800, piglets receiving a basal diet plus oral dose infused with 1×10^{10} CFU WB800 and ETEC K88; ETEC+WB800-KR32, piglets receiving a basal diet plus oral dose infused with 1×10^{10} CFU WB800-KR32 and ETEC K88 (grouping information, the same below). ETEC, enterotoxigenic *Escherichia coli*; CFU, colony forming units; CAT, catalase; T-AOC, total antioxidant capacity; SOD, superoxide dismutase; MDA, malondialdehyde; GPx, glutathione peroxidase; prot: protein; ns, not significant.

3.3 Antioxidant-related gene expression

Compared with the CON group, the messenger RNA (mRNA) expression of *CAT* was not significantly different from the ETEC group (P>0.1; Fig. 3a). Compared with the CON group, ETEC infection upregulated the mucosal *GPx*, *Nrf2*, and *SOD1* mRNA abundance in the ileum; pretreatment with WB800-KR32 could reverse the mRNA expression of *GPx*, *Nrf2*, and *SOD1* in ileal mucosae (Figs. 3b, 3d, and 3e). The mRNA expression of *Keap1* was inconsistent in the jejunum and ileum of the ETEC group. Compared with the CON group, the mRNA expression of *Keap1* was significantly upregulated in the ileum of piglets in the ETEC group; meanwhile, pretreatment with WB800-KR32 could alleviate the increment induced by ETEC infection in the ileum (P<0.05; Fig. 3c).

3.4 Antioxidant-related protein expression

Compared with the CON group, the Nrf2 protein was significantly decreased in the ETEC and ETEC+WB800 groups, and the Keap1 protein was significantly increased in the ETEC and ETEC+WB800 groups; pretreatment with WB800-KR32 could reverse these changes and resulted in no significant difference compared with the CON group (Fig. 4).

3.5 Fecal microbial community

Across all 21 samples, 978 683 high-quality sequences were identified, with an average length of 413.84 bp. Compared with the Day 1 group, the OTUs (Sobs) and richness estimators (Ace and Chao) were significantly increased on Days 14 and 17 (P<0.05; Figs. 5a, 5d, and 5e). Besides, no remarkable differences were found in the diversity indices (Shannon and Simpson) (Figs. 5b and 5c).

We further investigated the shifts in bacterial taxa that were caused by oral WB800-KR32 (prior to WB800-KR32 and post-WB800-KR32 treatment for 14 d) and ETEC infection (3 d post-ETEC K88 infection). PCoA based on Bray-Curtis distance revealed the distinct clustering of microbiota composition for the three groups (Fig. 6a). The analysis of similarities in Bray-Curtis distance indicated that oral WB800-KR32 and ETEC infection tended to be different (P=0.001) with an R^2-value of 0.2315, suggesting that the microbiota of the three groups were different. NMDS ordination plot based on the Bray-Curtis distance metric showed that the fecal bacterial communities in the samples could be differentiated by oral WB800-KR32 and ETEC infection (Fig. 6b). The overall microbial composition of the three groups differed at the class level.

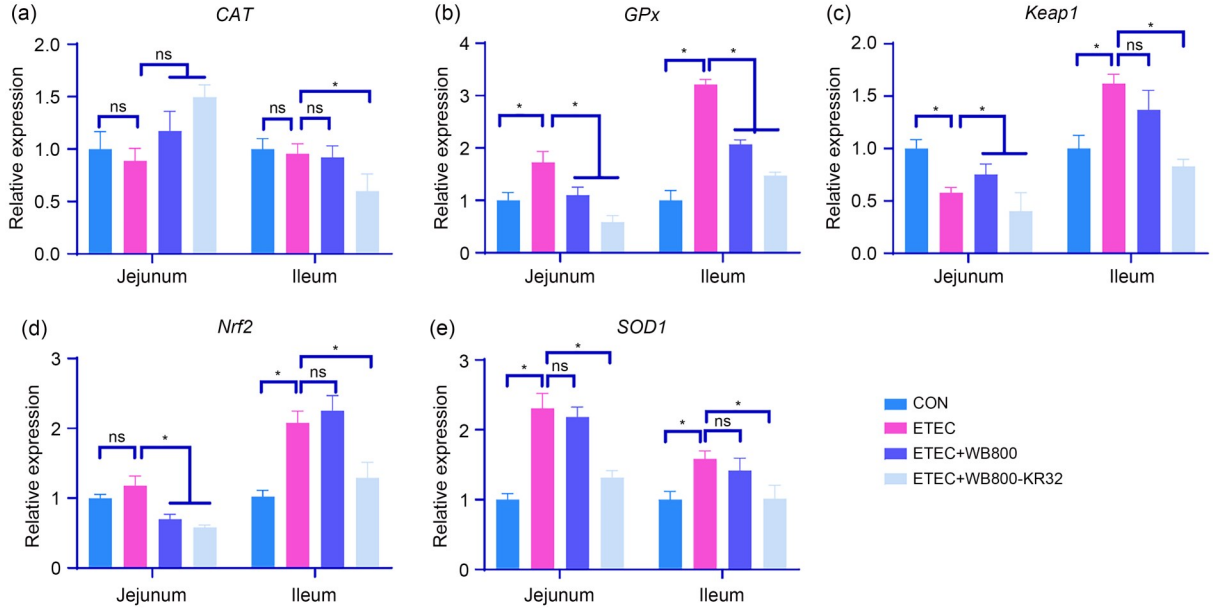

Fig. 3 Effects of pretreatment with WB800-KR32 on the relative mRNA levels of antioxidant-related genes (*CAT* (a), *GPx* (b), *Keap1* (c), *Nrf2* (d), *SOD1* (e)) in the mucosae of jejunum and ileum in weaned piglets infected with ETEC K88. The results were expressed as mean±standard error of the mean (SEM), n=7. * P<0.05, ^{ns} P>0.1. mRNA, messenger RNA; ETEC, enterotoxigenic *Escherichia coli*; *CAT*, catalase; *GPx*, glutathione peroxidase; *Keap1*, Kelch-like ECH-associated protein 1; *Nrf2*, nuclear factor erythroid 2-related factor 2; *SOD1*, superoxide dismutase 1; ns, not significant.

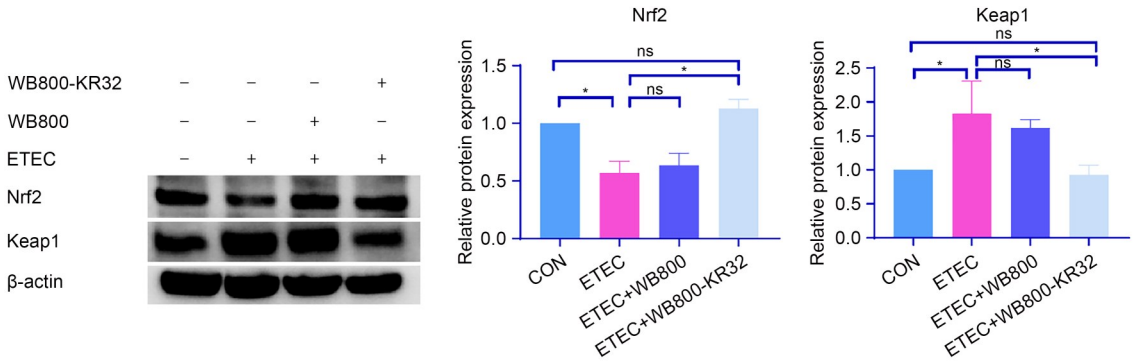

Fig. 4 Effects of pretreatment with WB800-KR32 on the antioxidant-related proteins (Nrf2 and Keap1) in ileal mucosa in weaned piglets infected with ETEC K88. The results were expressed as mean±standard error of the mean (SEM), *n*=7. * *P*<0.05, ns *P*>0.1. Nrf2, nuclear factor erythroid 2-related factor 2; Keap1, Kelch-like ECH-associated protein 1; ETEC, enterotoxigenic *Escherichia coli*; ns, not significant.

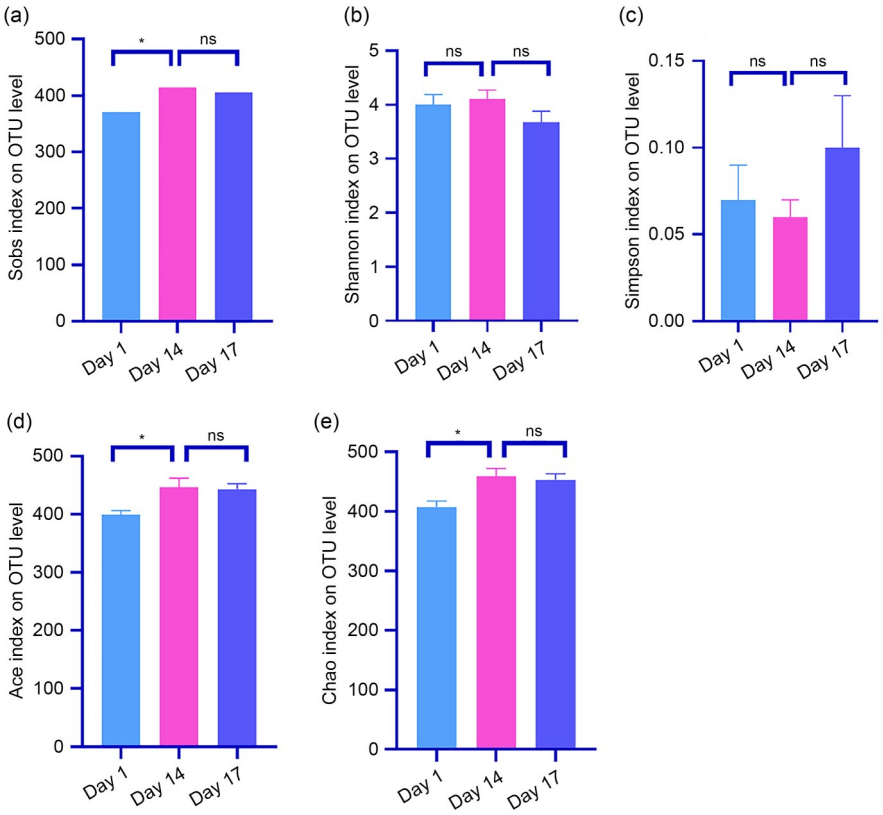

Fig. 5 Effects of treatment with WB800-KR32 and ETEC K88 on the alpha-diversity Sobs (a), Shannon (b), Simpson (c), Ace (d), and Chao (e) of fecal microbiota. The results were expressed as mean±standard error of the mean (SEM), *n*=7. * *P*<0.05, ns *P*>0.1. ETEC, enterotoxigenic *Escherichia coli*; OTU: operational taxonomic unit; ns, not significant.

The five largest classes represented in each group were Clostridia, Bacteroidia, Bacilli, Spirochaetia, and Negativicutes (Fig. 6c). The abundance of Clostridia gradually increased in response to treatment with WB800-KR32 and ETEC. The abundance of Bacteroidia was significantly decreased after WB800-KR32 treatment for 14 d and significantly increased 3 d after ETEC infection. The abundance of Bacilli was significantly increased after WB800-KR32 treatment and significantly decreased after ETEC infection. At the species level, *Eubacterium_rectale_ATCC_33656* was significantly increased in the Day 14 group (Fig. 6d). We found that multiple KEGG (level 3) categories were disturbed (Figs. 6e and 6f). Specifically, the enriched

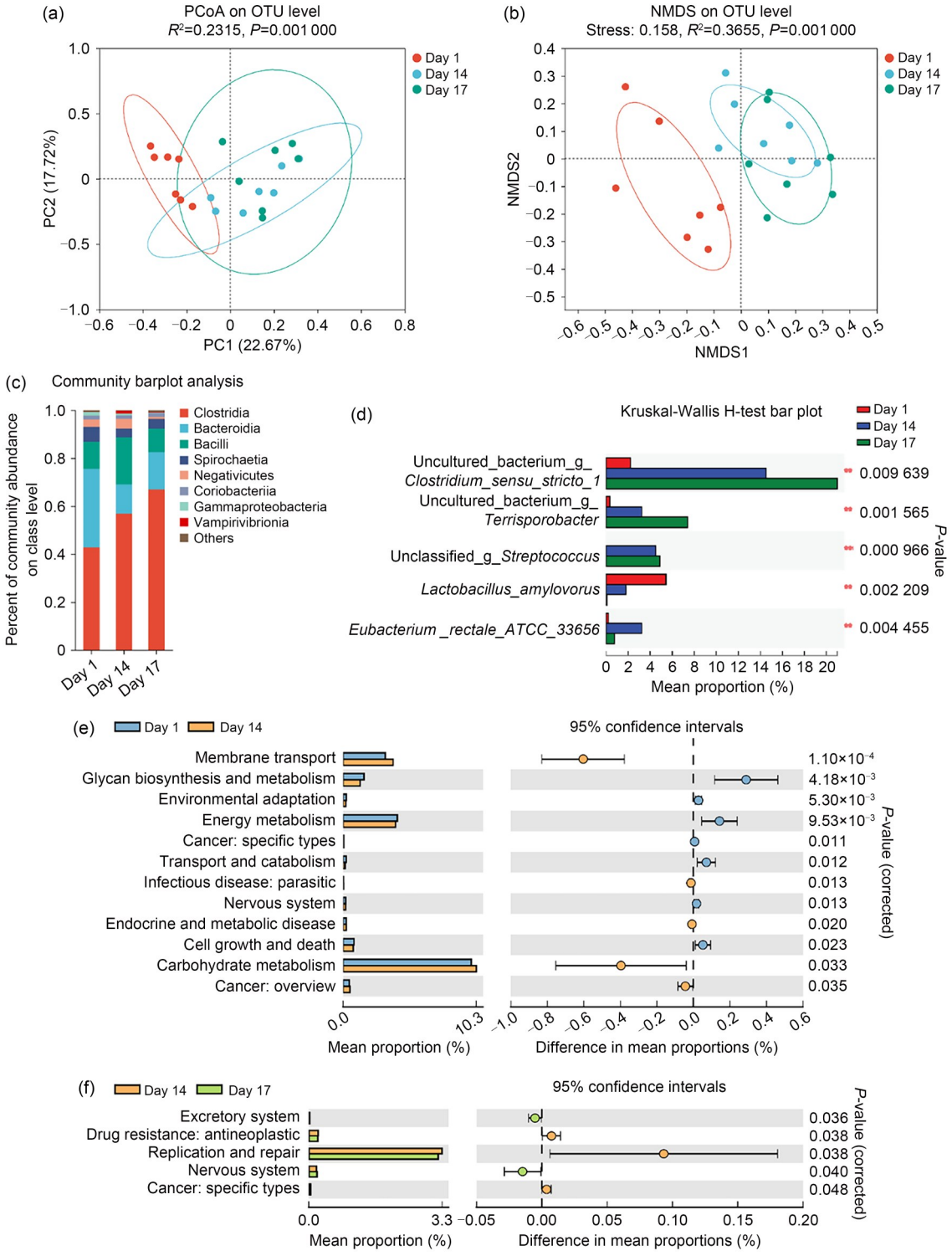

Fig. 6 Effects of treatment with WB800-KR32 and ETEC K88 on fecal microbial composition and function. (a) PCoA analysis based on the Bray-Curtis distance metric. (b) NMDS ordination analysis of fecal bacterial communications in the Days 1, 14, and 17 groups based on Bray-Curtis distance metric. (c) Class-level compositions of bacterial community. (d) Top 5 significantly different species between the groups. (e) Significantly different pathways enriched at KEGG level 3 (Days 1 vs. 14). (f) Significantly different pathways enriched at KEGG level 3 (Days 14 vs. 17). ETEC, enterotoxigenic *Escherichia coli*; PCoA, principal coordinates analysis; NMDS, nonmetric multidimensional scaling; KEGG, Kyoto Encyclopedia of Genes and Genomes; OTU, operational taxonomic unit; PC, principal component.

pathways were membrane transport, glycan biosynthesis and metabolism, energy metabolism, and carbohydrate metabolism. Membrane transport and carbohydrate metabolism were significantly upregulated in the Day 14 group compared with Day 1 (Fig. 6e). Replication and repair, as well as "drug resistance: antineoplastic" were significantly upregulated in the Day 14 group compared with Day 17 (Fig. 6f).

4 Discussion

The intestinal mucosa is the main tissue of defense against various pathogens in the intestinal lumen (Smith et al., 2010). However, it is easily attacked by different pathogenic bacteria in the weaning period, as the immune and antioxidant systems are not yet well-developed at this time (Yin et al., 2014). Intestinal oxidative damage induced by ETEC is regarded as a severe health concern and is a main factor of morbidity and mortality in animals. KR32 is an AMP that has been reported to exert high antimicrobial activity in vitro and decrease the inflammatory response in vivo. The present study revealed that the therapeutic administration of WB800-KR32 improved host defense against ETEC K88 invasion-induced intestinal oxidative damage.

The antioxidant and oxidant systems are normally in dynamic balance. Reactive oxygen species (ROS) are produced during cellular metabolism, while perturbations in the balance of antioxidants and the reactive species can lead to alterations in cell composition and the potential damage of cellular activities, collectively named as "oxidative stress." The effectiveness of the first line of antioxidants including CAT, SOD, and GPx is vital for the whole defense strategy, especially against ROS that are perpetually generated during normal body metabolism. CAT is one of the essential antioxidant enzymes that alleviate oxidative stress to a substantial extent by destroying cellular hydrogen peroxide (Nandi et al., 2019), which underlines its importance in the aforementioned physiological processes (Ighodaro and Akinloye, 2018). The malfunction of CAT has been postulated to be linked to the pathogenesis of many pathogen infections (Guan et al., 2019; Yu et al., 2021). In the present study, ETEC challenge significantly reduced the serum activity of CAT and the T-AOC, indicating the disruption of the body's antioxidant capacity.

Furthermore, we detected the antioxidant enzyme and byproduct in the small intestine mucosa. The results showed that ETEC infection had a little effect on duodenum mucosa, which was in agreement with a previous study (Xie et al., 2021). Therefore, we emphatically examined the antioxidant capacity of jejunum and ileum in subsequent experiments. ETEC challenge did not affect the activity of CAT; however, pretreatment with WB800-KR32 significantly enhanced it in the ileum. It was suggested that our recombinant bacteria exerted a protective effect after ETEC infection. T-AOC was significantly decreased after ETEC challenge, and reached a normal condition with the pretreatment of WB800-KR32 but not WB800, indicating that WB800 had no effect on mucosal antioxidant activity, while the recombinant bacteria WB800-KR32 improved intestinal antioxidant activity through secreting the AMP KR32. The MDA content was significantly increased after ETEC infection in previous studies (Guan et al., 2019; Xiong et al., 2020; Wu et al., 2021), whereas it was alleviated by WB800-KR32 in our study. It was suggested that WB800-KR32 could decrease the mucosal lipid peroxide on account of MDA as the main product of lipid peroxidation produced from polyunsaturated fatty acids (Tsikas, 2017). GPx is well-known for its antioxidant and anti-inflammatory activity, and is highly expressed in the crypt-to-villus axis that secretes microbicidal defensins in response to bacteria (Esworthy et al., 1998; Ayabe et al., 2000; Florian et al., 2001). Increased GPx activity inhibits hydroperoxide-mediated apoptosis (Chu et al., 2004), while insufficient GPx activity induces acute and chronic inflammation in the mucosal epithelium. In our study, the activity of GPx was significantly decreased in response to ETEC infection, which was alleviated by WB800-KR32. This finding indicated that pretreatment with WB800-KR32 could improve mucosal antioxidant level.

Previous studies found that ETEC invasion leads to the upregulation of antioxidant genes (Xie et al., 2021; Yu et al., 2021). Based on the results of antioxidant enzyme activity in the jejunal and ileal mucosae, we examined the mRNA expression of *CAT* and *GPx*. The results showed that compared with ETEC group, the relative expression of *CAT* was significantly decreased in response to pretreatment with WB800-KR32. On the other hand, the expression of *GPx* was elevated by ETEC infection and reversed by WB800-KR32. *GPx1* knockout is more susceptible to oxidative challenge

(Xia et al., 2021), which may explain that WB800-KR32 reduced the ROS while suppressing the expression of antioxidant-related genes. The deficiency and mutation of *CAT* has been associated with various diseases and abnormalities (Góth et al., 2004). Members of the SOD family to neutralize the first oxygen-derived ROS are the most powerful antioxidants in the cell, providing protection against bacterial infection (Wu et al., 2021). An association between SOD deficiency and many pathologies has been found in animals and human beings (Ighodaro and Akinloye, 2018); therefore, this enzyme seems indispensable to cellular health, protecting cells from excessive oxygen radicals and free radicals. The expression of SOD was significantly upregulated during oxidative stress (Wen et al., 2020a), which is consistent with our results.

In a healthy cell, Nrf2 is anchored to the cytoskeleton of actin in the form of Keap1-Nrf2 complex. In the cytoplasm, the complex is inactivated by ubiquitination to maintain its low concentration and stable state (Lyakhovich et al., 2006). The Nrf2 pathway is activated by the specific stimulation of defense mechanism such as oxidative stress. Under oxidative stress, however, the cysteine residues of Keap1 are oxidized and Nrf2 is allowed to dissociate from the inhibitory complex (Wu et al., 2012). Therefore, we detected the mRNA expression of *Nrf2* and *Keap1*. The results showed that ETEC infection upregulated the mRNA expression of both *Keap1* and *Nrf2*, which was reversed by WB800-KR32. These results suggested that ETEC could trigger oxidative stress, and our recombinant bacteria decreased the oxidative response. We further detected the protein expression of Nrf2 and Keap1, which revealed that ETEC infection significantly downregulated the protein expression of Nrf2, while it significantly upregulated the expression of Keap1. Meanwhile, this effect was reversed by pretreatment with WB800-KR32, suggesting that WB800-KR32 exerted a protective effect on intestinal oxidative damage by mediating through the Nrf2-Keap1 pathway.

The fecal microbiota analysis showed that WB800-KR32 had a considerable effect on taxonomic composition. The results for the Top 5 significantly different species showed that the abundance of uncultured_bacterium_g_*Clostridium_sensu_stricto_1* and uncultured_bacterium_g_*Terrisporobacter* was significantly increased on Days 14 and 17. *Clostridium* species possess potential probiotic characteristics important for intestinal homeostasis (Guo et al., 2020); uncultured_bacterium_g_*Clostridium_sensu_stricto_1*, referring to the *Clostridium* cluster I, was increased in colon fed with a low-protein diet in finishing pigs (Fan et al., 2017). Moreover, it was found that the participation of *Akkermansia muciniphila* promoted the increments of genera *Clostridium_sensu_stricto_1* in the jejunum of broilers, which was associated with necrotic enteritis development (Yang et al., 2022). Also, a diet enriched with *Pediococcus pentosaceus* significantly increased the genus level of *Clostridium_sensu_stricto_1* in finishing pigs (Liu et al., 2021). The treatment of chronic diarrhea patients with *Lactobaccilus plantarum* CCFM1143 (a probiotic) could mitigate the apparent clinical symptoms, accomplished through the enrichment of *Terrisporobacter* in feces (Yang et al., 2021). On the contrary, it has been found that flavor supplementation significantly decreased genera *Clostridium_sensu_stricto_1* and *Terrisporobacter*, while it improved the reproductive performance of sows (Wang et al., 2021). In addition, with the evolution of gut microbiota, the abundance of *Clostridium_sensu_stricto_1* and *Terrisporobacter* was increased on Days 60 and 75 compared to the younger stage in Ningxiang pigs (Li et al., 2021). *Eubacterium_rectale_ATCC_33656* was significantly increased after WB800-KR32 treatment, which is one of the acetate-converting butyrate producers (Riviere et al., 2015). Moreover, butyrate was demonstrated to be beneficial on intestinal homeostasis and energy metabolism. It also enhances intestinal barrier function owing to its anti-inflammatory properties (Liu et al., 2018). These data indicated that WB800-KR32 could protect intestinal health through increasing the relative abundance of butyrate producing bacteria *Eubacterium_rectale_ATCC_33656*. As the complexity of microbial communities makes it challenging to identify which genera or species are beneficial to host health, future studies may use Spearman's correlation analysis to further estimate the relationship with the apparent symptoms of host. AMPs are crucial for maintaining the balance of microbiota, which has therapeutic implications for infections by enteric pathogens (Zong et al., 2020). Therefore, further research is needed to investigate the potential benefits of such metabolites. The above findings highlight that WB800-KR32 may play a role in the prevention of ETEC-induced microbiota disruption.

5 Conclusions

Pretreatment with WB800-KR32 could alleviate ETEC K88 infection induced by intestinal oxidative injuries in weaned piglets acting through the Nrf2-Keap1 pathway, while microbiota might mediate this effect. The present study provides a new perspective for applying WB800-KR32 as potential therapeutics to regulate the intestinal oxidative balance after ETEC K88 infection.

Acknowledgments

This work was supported by the Zhejiang Provincial Key R&D Program of China (No. 2021C02008), the China Agriculture Research System of MOF and MARA (No. CARS-35), the National Natural Science Foundation of China (No. 32022079), the Fundamental Research Funds for the Central Universities (No. 2022QZJH46), and the Taishan Industrial Leading Talents Project.

Author contributions

Chaoyue WEN performed the experimental research and data analysis, and wrote and edited the manuscript. Hong ZHANG, Qiuping GUO, Yehui DUAN, Sisi CHEN, Mengmeng HAN, and Fengna LI contributed to the study design, data analysis, and writing and editing of the manuscript. Mingliang JIN designed the experiment, and wrote and revised the manuscript. Yizhen WANG contributed to the study design and editing of the manuscript. All authors have read and approved the final manuscript, and therefore, have full access to all the data in the study and take responsibility for the integrity and security of the data.

Compliance with ethics guidelines

Chaoyue WEN, Hong ZHANG, Qiuping GUO, Yehui DUAN, Sisi CHEN, Mengmeng HAN, Fengna LI, Mingliang JIN, and Yizhen WANG declare that they have no conflict of interest.

All institutional and national guidelines for the care and use of laboratory animals were followed. All animal procedures were approved by the Committee of the Institute of Subtropical Agriculture, the Chinese Academy of Sciences (No. ISA-2022-022).

References

Ayabe T, Satchell DP, Wilson CL, et al., 2000. Secretion of microbicidal α-defensins by intestinal Paneth cells in response to bacteria. *Nat Immunol*, 1(2):113-118. https://doi.org/10.1038/77783

Bäckhed F, Fraser CM, Ringel Y, et al., 2012. Defining a healthy human gut microbiome: current concepts, future directions, and clinical applications. *Cell Host Microbe*, 12(5):611-622. https://doi.org/10.1016/j.chom.2012.10.012

Chu FF, Esworthy RS, Doroshow JH, 2004. Role of Se-dependent glutathione peroxidases in gastrointestinal inflammation and cancer. *Free Radic Biol Med*, 36(12):1481-1495. https://doi.org/10.1016/j.freeradbiomed.2004.04.010

Cruz KCP, Enekegho LO, Stuart DT, 2022. Bioengineered probiotics: synthetic biology can provide live cell therapeutics for the treatment of foodborne diseases. *Front Bioeng Biotechnol*, 10:890479. https://doi.org/10.3389/fbioe.2022.890479

Duan YH, Zeng LM, Li FN, et al., 2017. Effect of branched-chain amino acid ratio on the proliferation, differentiation, and expression levels of key regulators involved in protein metabolism of myocytes. *Nutrition*, 36:8-16. https://doi.org/10.1016/j.nut.2016.10.016

Esworthy RS, Swiderek KM, Ho YS, et al., 1998. Selenium-dependent glutathione peroxidase-GI is a major glutathione peroxidase activity in the mucosal epithelium of rodent intestine. *Biochim Biophys Acta*, 1381(2):213-226. https://doi.org/10.1016/S0304-4165(98)00032-4

Fan PX, Liu P, Song PX, et al., 2017. Moderate dietary protein restriction alters the composition of gut microbiota and improves ileal barrier function in adult pig model. *Sci Rep*, 7:43412. https://doi.org/10.1038/srep43412

Florian S, Wingler K, Schmehl K, et al., 2001. Cellular and subcellular localization of gastrointestinal glutathione peroxidase in normal and malignant human intestinal tissue. *Free Radic Res*, 35(6):655-663. https://doi.org/10.1080/10715760100301181

Góth L, Rass P, Páy A, 2004. Catalase enzyme mutations and their association with diseases. *Mol Diagn*, 8(3):141-149. https://doi.org/10.1007/BF03260057

Guan GP, Ding SJ, Yin YL, et al., 2019. *Macleaya cordata* extract alleviated oxidative stress and altered innate immune response in mice challenged with enterotoxigenic *Escherichia coli*. *Sci China Life Sci*, 62(8):1019-1027. https://doi.org/10.1007/s11427-018-9494-6

Guilloteau P, Zabielski R, Hammon HM, et al., 2010. Nutritional programming of gastrointestinal tract development. Is the pig a good model for man? *Nutr Res Rev*, 23(1):4-22. https://doi.org/10.1017/S0954422410000077

Guo PT, Zhang K, Ma X, et al., 2020. *Clostridium* species as probiotics: potentials and challenges. *J Anim Sci Biotechnol*, 11:24. https://doi.org/10.1186/s40104-019-0402-1

Hu WY, Yang YY, Li Z, et al., 2019. Antibacterial, cytotoxicity and mechanism of the antimicrobial peptide KR-32 in weaning piglets. *Int J Pept Res Ther*, 26(2):943-953. https://doi.org/10.1007/s10989-019-09898-0

Huang JJ, Bai YM, Xie WT, et al., 2023. *Lycium barbarum* polysaccharides ameliorate canine acute liver injury by reducing oxidative stress, protecting mitochondrial function, and regulating metabolic pathways. *J Zhejiang Univ-Sci B (Biomed & Biotechnol)*, 24:157-171. https://doi.org/10.1631/jzus.B2200213

Ighodaro OM, Akinloye OA, 2018. First line defence antioxidants-superoxide dismutase (SOD), catalase (CAT) and glutathione peroxidase (GPX): their fundamental role in the entire antioxidant defence grid. *Alex J Med*, 54(4):287-293. https://doi.org/10.1016/j.ajme.2017.09.001

Jin ML, Zhang H, Zhao K, et al., 2018. Responses of intestinal mucosal barrier functions of rats to simulated weightlessness. *Front Physiol*, 9:729. https://doi.org/10.3389/fphys.2018.00729

Lekshmi M, Ammini P, Kumar S, et al., 2017. The food production environment and the development of antimicrobial resistance in human pathogens of animal origin. *Microorganisms*, 5(1):11. https://doi.org/10.3390/microorganisms5010011

Li FN, Duan YH, Li YH, et al., 2015. Effects of dietary *n*-6:*n*-3 PUFA ratio on fatty acid composition, free amino acid profile and gene expression of transporters in finishing pigs. *Br J Nutr*, 113(5):739-748. https://doi.org/10.1017/S0007114514004346

Li H, Ma LT, Li ZQ, et al., 2021. Evolution of the gut microbiota and its fermentation characteristics of Ningxiang pigs at the young stage. *Animals (Basel)*, 11(3):638. https://doi.org/10.3390/ani11030638

Li WF, Zhou XX, Lu P, 2004. Bottlenecks in the expression and secretion of heterologous proteins in *Bacillus subtilis*. *Res Microbiol*, 155(8):605-610. https://doi.org/10.1016/j.resmic.2004.05.002

Liu H, Wang J, He T, et al., 2018. Butyrate: a double-edged sword for health? *Adv Nutr*, 9(1):21-29. https://doi.org/10.1093/advances/nmx009

Liu HY, Cao XX, Wang H, et al., 2019. Antimicrobial peptide KR-32 alleviates *Escherichia coli* K88-induced fatty acid malabsorption by improving expression of fatty acid transporter protein 4 (FATP4). *J Anim Sci*, 97(6):2342-2356. https://doi.org/10.1093/jas/skz110

Liu SN, Zhang B, Xiang DC, et al., 2021. Effect of *Pediococcus pentosaceus* 368 on grow performance, fecal microbiota and metabolite in pigs. *Microbiol China*, 48(6):2035-2048 (in Chinese). https://doi.org/10.13344/j.microbiol.china.200898

Luan C, Zhang HW, Song DG, et al., 2014a. Expressing antimicrobial peptide cathelicidin-BF in *Bacillus subtilis* using SUMO technology. *Appl Microbiol Biotechnol*, 98(8):3651-3658. https://doi.org/10.1007/s00253-013-5246-6

Luan C, Xie YG, Pu YT, et al., 2014b. Recombinant expression of antimicrobial peptides using a novel self-cleaving aggregation tag in *Escherichia coli*. *Can J Microbiol*, 60(3):113-120. https://doi.org/10.1139/cjm-2013-0652

Luise D, Lauridsen C, Bosi P, et al., 2019. Methodology and application of *Escherichia coli* F4 and F18 encoding infection models in post-weaning pigs. *J Anim Sci Biotechnol*, 10:53. https://doi.org/10.1186/s40104-019-0352-7

Lyakhovich VV, Vavilin VA, Zenkov NK, et al., 2006. Active defense under oxidative stress. The antioxidant responsive element. *Biochemistry (Mosc)*, 71(9):962-974. https://doi.org/10.1134/S0006297906090033

Nandi A, Yan LJ, Jana CK, et al., 2019. Role of catalase in oxidative stress- and age-associated degenerative diseases. *Oxid Med Cell Longev*, 2019:9613090. https://doi.org/10.1155/2019/9613090

National Research Council, 2012. Nutrients Requirements of Swine, 11th Ed. National Academy Press, Washington, USA, p.20-26.

Rajput SA, Liang SJ, Wang XQ, et al., 2021. Lycopene protects intestinal epithelium from deoxynivalenol-induced oxidative damage via regulating Keap1/Nrf2 signaling. *Antioxidants*, 10(9):1493. https://doi.org/10.3390/antiox10091493

Ren M, Cai S, Zhou T, et al., 2019. Isoleucine attenuates infection induced by *E. coli* challenge through the modulation of intestinal endogenous antimicrobial peptide expression and the inhibition of the increase in plasma endotoxin and IL-6 in weaned pigs. *Food Funct*, 10(6):3535-3542. https://doi.org/10.1039/C9FO00218A

Riviere A, Gagnon M, Weckx S, et al., 2015. Mutual cross-feeding interactions between *Bifidobacterium longum* subsp. longum NCC2705 and Eubacterium rectale ATCC 33656 explain the bifidogenic and butyrogenic effects of arabinoxylan oligosaccharides. *Appl Environ Microbiol*, 81(22):7767-7781. https://doi.org/10.1128/AEM.02089-15

Roura E, Koopmans SJ, Lalles JP, et al., 2016. Critical review evaluating the pig as a model for human nutritional physiology. *Nutr Res Rev*, 29(1):60-90. https://doi.org/10.1017/S0954422416000020

Shi Y, Hu Y, Wang ZQ, et al., 2022. The Protective effect of taurine on oxidized fish-oil-induced liver oxidative stress and intestinal barrier-function impairment in juvenile *Ictalurus punctatus*. *Antioxidants*, 10(11):1690. https://doi.org/10.3390/antiox10111690

Smith F, Clark JE, Overman BL, et al., 2010. Early weaning stress impairs development of mucosal barrier function in the porcine intestine. *Am J Physiol Gastrointest Liver Physiol*, 298(3):G352-G363. https://doi.org/10.1152/ajpgi.00081.2009

Tang YL, Li FN, Tan B, et al., 2014. Enterotoxigenic *Escherichia coli* infection induces intestinal epithelial cell autophagy. *Vet Microbiol*, 171(1-2):160-164. https://doi.org/10.1016/j.vetmic.2014.03.025

Tsikas D, 2017. Assessment of lipid peroxidation by measuring malondialdehyde (MDA) and relatives in biological samples: analytical and biological challenges. *Anal Biochem*, 524:13-30. https://doi.org/10.1016/j.ab.2016.10.021

Wang J, Su LQ, Zhang L, et al., 2022. *Spirulina platensis* aqueous extracts ameliorate colonic mucosal damage and modulate gut microbiota disorder in mice with ulcerative colitis by inhibiting inflammation and oxidative stress. *J Zhejiang Univ-Sci B (Biomed & Biotechnol)*, 23(6):481-501. https://doi.org/10.1631/jzus.B2100988

Wang RJ, Liu N, Yang YC, et al., 2021. Flavor supplementation during late gestation and lactation periods increases

the reproductive performance and alters fecal microbiota of the sows. *Anim Nutr*, 7(3):679-687. https://doi.org/10.1016/j.aninu.2021.01.007

Wen CY, Li FN, Duan YH, et al., 2019. Dietary taurine regulates free amino acid profiles and taurine metabolism in piglets with diquat-induced oxidative stress. *J Funct Foods*, 62:103569. https://doi.org/10.1016/j.jff.2019.103569

Wen CY, Li FN, Guo QP, et al., 2020a. Protective effects of taurine against muscle damage induced by diquat in 35 days weaned piglets. *J Anim Sci Biotechnol*, 11:56. https://doi.org/10.1186/s40104-020-00463-0

Wen CY, Guo QP, Wang WL, et al., 2020b. Taurine alleviates intestinal injury by mediating tight junction barriers in diquat-challenged piglet models. *Front Physiol*, 11:449. https://doi.org/10.3389/fphys.2020.00449

Wen CY, Li SY, Wang JJ, et al., 2021. Heat stress alters the intestinal microbiota and metabolomic profiles in mice. *Front Microbiol*, 12:706772. https://doi.org/10.3389/fmicb.2021.706772

Wierup M, 2001. The Swedish experience of the 1986 year ban of antimicrobial growth promoters, with special reference to animal health, disease prevention, productivity, and usage of antimicrobials. *Microb Drug Resist*, 7(2): 183-190. https://doi.org/10.1089/10766290152045066

Wu T, Shi YT, Zhang YY, et al., 2021. *Lactobacillus rhamnosus* LB1 alleviates enterotoxigenic *Escherichia coli*-induced adverse effects in piglets by improving host immune response and anti-oxidation stress and restoring intestinal integrity. *Front Cell Infect Microbiol*, 11:724401. https://doi.org/10.3389/fcimb.2021.724401

Wu X, Zhang Y, Liu Z, et al., 2012. Effects of oral supplementation with glutamate or combination of glutamate and N-carbamylglutamate on intestinal mucosa morphology and epithelium cell proliferation in weanling piglets. *J Anim Sci*, 90(S4):337-339. https://doi.org/10.2527/jas.53752

Xia XJ, Zhang XL, Liu MC, et al., 2021. Toward improved human health: efficacy of dietary selenium on immunity at the cellular level. *Food Funct*, 12(3):976-989. https://doi.org/10.1039/D0FO03067H

Xia YY, Bin P, Liu SJ, et al., 2018. Enterotoxigenic *Escherichia coli* infection promotes apoptosis in piglets. *Microb Pathog*, 125:290-294. https://doi.org/10.1016/j.micpath.2018.09.032

Xia YY, Chen SY, Zhao YY, et al., 2019. GABA attenuates ETEC-induced intestinal epithelial cell apoptosis involving $GABA_AR$ signaling and the AMPK-autophagy pathway. *Food Funct*, 10(11):7509-7522. https://doi.org/10.1039/C9FO01863H

Xie WC, Song LY, Wang X, et al., 2021. A bovine lactoferricin-lactoferrampin-encoding *Lactobacillus reuteri* CO21 regulates the intestinal mucosal immunity and enhances the protection of piglets against enterotoxigenic *Escherichia coli* K88 challenge. *Gut Microbes*, 13(1):1956281. https://doi.org/10.1080/19490976.2021.1956281

Xiong W, Huang J, Li XY, et al., 2020. Icariin and its phosphorylated derivatives alleviate intestinal epithelial barrier disruption caused by enterotoxigenic *Escherichia coli* through modulate p38 MAPK in vivo and in vitro. *FASEB J*, 34(1):1783-1801. https://doi.org/10.1096/fj.201902265R

Yang B, Yue Y, Chen Y, et al., 2021. *Lactobacillus plantarum* CCFM1143 alleviates chronic diarrhea *via* inflammation regulation and gut microbiota modulation: a double-blind, randomized, placebo-controlled study. *Front Immunol*, 12: 746585. https://doi.org/10.3389/fimmu.2021.746585

Yang WY, Chou CH, Wang C, 2022. The effects of feed supplementing *Akkemansia muciniphila* on incidence, severity, and gut microbiota of necrotic enteritis in chickens. *Poult Sci*, 101(4):101751. https://doi.org/10.1016/j.psj.2022.101751

Yin J, Wu MM, Xiao H, et al., 2014. Development of an antioxidant system after early weaning in piglets. *J Anim Sci*, 92(2):612-619. https://doi.org/10.2527/jas.2013-6986

Younis NS, Abduldaium MS, Mohamed ME, 2020. Protective effect of geraniol on oxidative, inflammatory and apoptotic alterations in isoproterenol-induced cardiotoxicity: role of the Keap1/Nrf2/HO-1 and PI3K/Akt/mTOR pathways. *Antioxidants*, 9(10):977. https://doi.org/10.3390/antiox9100977

Yu E, Chen DW, Yu B, et al., 2021. Amelioration of enterotoxigenic *Escherichia coli*-induced disruption of intestinal epithelium by *manno*-oligosaccharide in weaned pigs. *J Funct Foods*, 82:104492. https://doi.org/10.1016/j.jff.2021.104492

Zhang QS, Widmer G, Tzipori S, 2013. A pig model of the human gastrointestinal tract. *Gut Microbes*, 4(3):193-200. https://doi.org/10.4161/gmic.23867

Zhou J, Xiong X, Yin J, et al., 2019. Dietary lysozyme alters sow's gut microbiota, serum immunity and milk metabolite profile. *Front Microbiol*, 10:177. https://doi.org/10.3389/fmicb.2019.00177

Zong X, Fu J, Xu BC, et al., 2020. Interplay between gut microbiota and antimicrobial peptides. *Anim Nutr*, 6(4):389-396. https://doi.org/10.1016/j.aninu.2020.09.002

Supplementary information

Fig. S1